HHS Public Access

Author manuscript

Circ Arrhythm Electrophysiol. Author manuscript; available in PMC 2021 December 01.

Published in final edited form as:

Circ Arrhythm Electrophysiol. 2020 December ; 13(12): e008912. doi:10.1161/CIRCEP.120.008912.

Personalized Digital-heart Technology for Ventricular Tachycardia Ablation Targeting in Hearts with Infiltrating Adiposity

Eric Sung, BA[1,4], **Adityo Prakosa, PhD**[1,4], **Konstantinos N. Aronis, MD**[2,4], **Shijie Zhou, PhD**[1,4], **Stefan L. Zimmerman, MD**[3,4], **Harikrishna Tandri, MD**[2,4], **Saman Nazarian, MD, PhD**[5], **Ronald D. Berger, MD, PhD**[2,4], **Jonathan Chrispin, MD**[2,4], **Natalia A. Trayanova, PhD**[1,4]

[1]Department of Biomedical Engineering, Johns Hopkins University

[2]Section of Cardiac Electrophysiology, Division of Cardiology, Department of Medicine, Johns Hopkins Hospital, Baltimore, MD

[3]Department of Radiological Sciences, Johns Hopkins Hospital, Baltimore, MD

[4]Alliance for Cardiovascular Diagnostic & Treatment Innovation, Johns Hopkins University

[5]Division of Cardiology, Perelman School of Medicine, University of Pennsylvania, Philadelphia, PA

Abstract

Background -—Infiltrating adipose tissue (inFAT) is a newly recognized pro-arrhythmic substrate for post-infarct ventricular tachycardias (VT) identifiable on contrast-enhanced computed tomography (CE-CT). This study presents novel digital-heart technology that incorporates inFAT from CE-CT to non-invasively predict VT ablation targets and assesses the capability of the technology by comparing its predictions with VT ablation procedure data from patients with ischemic cardiomyopathy (ICM).

Methods -—Digital-heart models reflecting patient-specific inFAT distributions were reconstructed from CE-CTs. The Digital-heart Identification of Fat-based Ablation Targeting (DIFAT) technology evaluated the rapid-pacing-induced VTs in each personalized inFAT-based substrate. DIFAT targets that render the inFAT substrate non-inducible to VT, including VTs that arise post-ablation, were determined. DIFAT predictions were compared to corresponding clinical ablations to assess the capabilities of the technology.

Results -—DIFAT was developed and applied retrospectively to 29 ICM patients with CE-CTs. DIFAT ablation volumes were significantly less than the estimated clinical ablation volumes (1.87 ± 0.35 cm^3 vs. 7.05 ± 0.88 cm^3, $p<0.0005$). DIFAT targets overlapped with clinical ablations in

Correspondence: Natalia A. Trayanova, PhD, FHRS, FAHA, Murray B. Sachs Endowed, Professor of Biomedical Engineering and Medicine, Director, Alliance for Cardiovascular Diagnostic and Treatment Innovation, Johns Hopkins University, 3400 N. Charles Street, Baltimore MD 21218, Tel: 410-516-4375, ntrayanova@jhu.edu.

Disclosures: None

79% of patients, mostly in the apex (72%) and inferior/inferolateral (74%). In 3 patients, DIFAT targets co-localized with redo ablations delivered years after the index procedure.

Conclusions -—DIFAT is a novel digital-heart technology for individualized VT ablation guidance designed to eliminate VT inducibility following initial ablation. DIFAT predictions co-localized well with clinical ablation locations but provided significantly smaller lesions. DIFAT also predicted VTs targeted in redo procedures years later. As DIFAT uses widely accessible CT, its integration into clinical workflows may augment therapeutic precision and reduce redo procedures.

Graphical Abstract

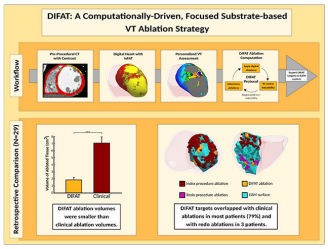

Keywords

computer-based model; cardiac computed tomography; catheter ablation; ischemic cardiomyopathy; lipomatous metaplasia; digital heart; ventricular tachycardia; fat deposition; Catheter Ablation and Implantable Cardioverter-Defibrillator; Arrhythmias; Electrophysiology

Introduction

Post-infarct ventricular tachycardia (VT) is a life-threatening arrhythmia resulting from re-entrant circuits formed by heterogeneous scarring. Catheter ablation, a mainstay of VT treatment[1], aims to disrupt these circuits. However, VT recurrence is common[2] in part due to imprecise ablation targeting of critical VT sites.[3] These limitations persist despite the development of new methodologies such as high-density mapping [4] and image-guided approaches.[5]

We previously developed a non-invasive, computationally-driven approach to guide VT ablation termed Virtual-heart Arrhythmia Ablation Targeting (VAAT), which was successfully tested in a retrospective study and in a small, multicenter prospective cohort.[6] Late gadolinium-enhanced cardiac magnetic resonance imaging (LGE-CMR)-defined myocardial scar and gray zone[5] were incorporated into personalized digital replicas of the heart's electrical function (digital hearts). VAAT identified optimal ablation sites in the post-infarct heart that eliminated all potential arrhythmias the substrate could sustain. VAAT further predicted the patient heart's response to the applied ablations, identifying whether new VT substrate emerged post-ablation.

High-quality LGE-CMR images are critical to VAAT because low image quality precludes adequate reconstruction of ventricular geometry and the distribution of structural remodeling, and thus can lead to inaccurate ablation target predictions. LGE-CMR often has

poor image quality due to artifacts and can be difficult to obtain clinically due to technical limitations[5], especially for patients with implantable cardioverter defibrillators (ICDs). Computed tomography (CT) can be readily acquired for patients with ischemic cardiomyopathy (ICM) and unlike LGE-CMR, has better image quality for patients with and without ICDs.[5] Delayed-enhancement CT localizes scar[7], but has insufficient image quality[8] necessary for scar reconstruction. Contrast-enhanced CT (CE-CT) provides excellent myocardial wall resolution[9], but cannot reveal scar distribution. Unlike myocardial scar, infiltrating adipose tissue (inFAT) is readily detected on CE-CT.[10,11] Importantly, post-infarct inFAT has recently been implicated as a pro-arrhythmic substrate that may contribute to VT.[12–14]

In this study, we propose novel CT-based digital-heart technology for VT ablation targeting in ICM patients based on personalized assessment of the arrhythmogenic propensity of remodeled substrate arising from inFAT penetration. The technology is advantageous as it uses widely accessible CTs as the imaging modality, making it implementable in centers without LGE-CMR expertise, and avoiding issues of LGE-CMR acquisition in patients with ICDs. Similar to VAAT, our new approach not only eliminates the inFAT-based substrate's arrhythmogenic propensity, but also anticipates the potential arrhythmogenic effects of ablation lesions on the substrate and takes this into account in determining the optimal set of VT ablation targets. This set of targets can be imported into electroanatomical mapping (EAM) systems, and the approach readily integrated into workflows to improve therapeutic precision of VT ablation and mitigate the need for redo ablations in VT recurrences.

The goal of this study is to present our new digital-heart approach, which we term DIFAT: Digital-heart Identification of Fat-based Ablation Targeting, and to retrospectively assess the feasibility of the technology in guiding VT ablation in patients with ICM by comparing the digital-heart predictions with clinical data.

Methods

The technology involves creating three-dimensional (3D) digital heart models from CE-CTs of patients with ICM reflecting the personalized inFAT distribution in the left ventricle (LV). The arrhythmogenicity of each patient's inFAT-based substrate is non-invasively assessed by analyzing its VT inducibility. DIFAT targets, which render the inFAT-based substrate non-inducible for VT from any pacing site, are next determined for each digital heart, including those that eliminate VT inducibility following initial ablation. The DIFAT workflow is presented in Fig.1. To assess DIFAT's ability to guide VT ablation, in this retrospective study, digital-heart predictions were compared with patient ablation procedure data.

Data presented here are available from the corresponding author upon request.

Study Population

We retrospectively enrolled 29 patients through the Johns Hopkins VT registry (approved by the institutional review board) from 2012 to 2018. Patients were selected randomly prior to reviewing any imaging or EAM data. Inclusion criteria were history of ICM and VT, VT ablation procedure performed using the Biosense Webster EAM system, and CE-CT

obtained within 1 month prior to index ablation. For patients with multiple CTs, CE-CTs from the time of the earliest procedure were used. CE-CTs were acquired using an established protocol.[13,15]

inFAT Identification on CE-CT Images

Details about CE-CT image processing workflow are presented in Supplementary Fig.1. The myocardium was segmented (Fig.1 top) as in previous studies.[6,16] inFAT in the post-infarct LV is pathologic whereas adipose tissue in the right ventricle (RV) could be physiologic.[11] Because of this distinction, RV inFAT was intentionally not identified. inFAT was identified as CE-CT signal intensity in the range −180 to −50 HU.[13,14] Previous studies have included hypoattenuated voxels with intensities >−50 HU as part of adipose tissue[13,15], but these likely represent an admixture of adipose and myocardial tissues.[17] Thus, tissues with intensity from −50 to −5 HU were distinguished separately from inFAT and termed “fat-myocardium admixture”, analogous to gray zone identified on LGE-CMR.[5]

To assess the spatial distribution, the inFAT volume in each of 4 regions (septum, apex, anterior/anterolateral, and inferior/inferolateral) was computed for each patient. A schematic of the anatomical regions is in Supplementary Fig.2. To account for heart size variability, the amount of inFAT within each anatomical region was determined as a percentage of total myocardial volume.

Personalized Digital Heart Reconstruction

3D heart models (digital hearts) of the post-infarct LV were reconstructed from the segmented myocardium along with the patients’ distributions of inFAT and fat-myocardium admixture (Fig.1 top). RV was not reconstructed because RV inFAT was excluded from consideration. To execute simulations, finite-element ventricular meshes were generated (Materialise Mimics) with ~5 million nodes with an average resolution of ~390 μm. Fiber orientations, specific to the individual LV, were assigned to each computational mesh on a per-element basis, as in previous publications[6,16], using a validated rule-based method.[18]

Assigning Electrophysiology Properties in inFAT Digital Hearts

inFAT was modeled as a non-conducting insulator. The electrophysiological effects of inFAT on surrounding ventricular tissue (i.e. fat-myocardium admixture) are poorly understood. Evidence suggests that gap junction remodeling[12], decreased conduction velocity[12,19], and altered electrogram signals[13,14] occur in fat-myocardium admixture, similar to electrophysiological changes in infarct border zone[20], however the extent of these changes remains unknown. In the absence of such data, the electrophysiological properties of fat-myocardium admixture were approximated with those of peri-infarct zone, the latter presented in our previous publications.[6,16] Non-diseased myocardium conductivity and action potential dynamics were the same as in our previous works.[6,16]

VT Inducibility in the Personalized inFAT Digital Heart Substrate

A previously validated rapid pacing protocol[6,16] tested VT inducibility in the personalized digital hearts. At each pacing site, six stimuli were delivered at 450-ms basic cycle length followed by successive premature stimuli until VT induction. Pacing was delivered

sequentially from 7 pacing sites, as done in previous work[21], striking a balance between assessing substrate arrhythmogenicity and ensuring the computational load can accommodate the clinical workflow timeline.

Induced VT in the inFAT-based digital heart substrate was defined as re-entry sustaining at least two cycles at the same critical site, as in previous studies[6,16] An example of an induced digital-heart VT is shown in Supplementary Fig.3. All simulations were performed using CARP (https://carp.medunigraz.at/).

Determining DIFAT Targets in the Personalized Digital Heart

After all VTs that the digital heart substrate can sustain were determined (Fig.1, top), VTs were analyzed for critical sites and DIFAT targeting. The DIFAT flowchart is presented in Fig.1 bottom; these targets are designed to result in non-inducibility of the inFAT-based substrate. Minimal-size (smallest volume needed to terminate VTs) digital ablation lesions were modeled as insulators and applied at the entrance, exit, or isthmus (depending on the geometry of inFAT and admixture regions) of all critical VT sites. As ablating VT could result in post-ablation arrhythmogenicity[22], the VT induction protocol was repeated in the post-ablated digital heart, to assess whether residual inFAT and admixture regions combine with ablation lesions to form new arrhythmogenic substrate. Emergent VTs in the modified digital substrate were virtually ablated, and this procedure was repeated until VTs could no longer be induced (Fig.1, bottom).

Retrospective Study: Comparing DIFAT Ablations with Clinical Ablation Procedural Data

To evaluate DIFAT's capability to determine VT ablation targets in post-infarction substrates, data was acquired from the ablation procedures of 29 patients: EAM data, ablation locations, and if available, anatomical data (CT angiography surfaces and/or landmarks defined by mapping/ultrasound) registered intraprocedually to the EAM surface. Details about our institution's ablation protocol can be found in the Supplementary Methods. To compare DIFAT's predictions with clinical data, EAM surfaces and clinical ablation locations were registered to the patient's digital heart using available anatomical data. Details about the registration process are in Supplementary Methods. An illustration of this process is in Supplementary Fig.4.

Once registered, all voltage maps and clinical ablation locations from both index and redo procedures were projected to the closest corresponding point on the digital heart endocardium. To compare DIFAT ablations with clinical ablations, clinical ablation lesion sizes needed to be estimated, as only catheter tip locations were known. An illustration of the estimated clinical lesions is in Supplementary Fig.5. The percentage of overlap between estimated clinical and DIFAT lesions in the 4 anatomical regions was determined for each patient.

Statistical Analyses

To compare inFAT distributions (Supplementary Fig.2), a non-parametric Friedman test was conducted to account for dependencies across anatomical regions and the non-normal distribution of inFAT across patients. A post-hoc analysis was performed to determine

specific differences in inFAT distribution among anatomical regions. The correlation between locations of DIFAT lesion volume with locations of EAM-defined scar was assessed using Fisher's exact test. Details can be found in Supplementary Materials. Total DIFAT and estimated clinical ablation volumes were compared using a paired t-test.

Results

Patient characteristics

Patient characteristics are summarized in Table 1. All 29 patients had implanted ICDs. Infarct location was anterior/anteroseptal for 11 patients (37.9%), inferior for 11 (37.9%), lateral for 5 (17.2%), and unknown for 2 (6.9%). Most patients (93.1%) received predominantly substrate-based ablations.

inFAT localizes primarily to the apex

The prevalence of inFAT is presented in Supplementary Fig.6. inFAT and fat-myocardium admixture were present in all patients, with medians (IQR) of 0.81% (1.25%) for inFAT and 3.02% (3.27%) for fat-myocardium admixture. Supplementary Table 1 provides each patient's infarct location and the predominant inFAT location; inFAT locations were concordant with infarct locations. The inFAT distributions across anatomical regions are summarized in Fig.2A. The largest and smallest amounts of inFAT were at the apex and the septum, respectively (Fig.2A). There were significant differences between inFAT amounts in the 4 anatomical regions ($p<0.005$). The median inFAT amount was 0.04% in septum, 0.25% in apex, 0.09% in anterior/anterolateral, and 0.14% in inferior/inferolateral (Fig.2A). Patients had more inFAT in apex than in anterior/anterolateral ($p<0.05$). Patients had less inFAT in septum than in apex ($p<0.05$) and inferior/inferolateral ($p<0.05$) (Fig.2A).

inFAT distribution varies highly across patients

Fig.2B illustrates the inFAT distribution patterns across patients. Patient 2 had inFAT in the apex and anterior whereas patient 3 had inFAT throughout the inferior. Patient 5 had a patchy distribution of inFAT and fat-myocardium admixture in the lateral/anterolateral. Patient 7's inFAT distribution was also patchy with a variable extent of inFAT into the mid-myocardium in the lateral/inferolateral.

inFAT and fat-myocardium admixture distribution determines VT circuits in digital hearts

The patient-specific inFAT and fat-myocardium admixture determined the VT circuits in digital hearts. Fig.3 presents examples of VTs in digital hearts of patients 1 and 2. For patient 1, three distinct VTs were induced. The inFAT and mitral annulus formed inexcitable obstacles, facilitating formation and maintenance of VT 1 (Fig.3 top left). VTs 2 and 3 involved propagation through two separate conduction channels formed by inFAT and fat-myocardium admixture in mid inferior (Fig.3 middle and bottom left). For patient 2, extensive inFAT and fat-myocardium admixture in the anterior and apex harbored three VT circuits. VT 1 was a macro-reentrant circuit (Fig.3 top right). VT 2 was located within the apical lateral inFAT-based substrate (Fig.3, middle right), whereas VT 3 localized to the apical septal inFAT periphery (Fig.3, bottom right).

DIFAT ablations co-localize with EAM-defined scar and clinical substrate modification lesions but have a much smaller volume

Because DIFAT is a more focused substrate-based VT ablation, we expected that DIFAT lesions would partially co-localize with clinical substrate modification lesions but have volumes smaller than the (estimated) clinical lesion volumes. Results confirmed this expectation, as shown in Fig.4 (1.87±0.35 cm^3 vs. 7.05±0.88 cm^3, $p<0.0005$).

DIFAT lesions were more likely to be found in scar than in border zone or healthy tissue (OR: 3.10 (2.95 to 3.27), $p<0.0005$). DIFAT lesions co-localized with clinical ablation lesions for 79% of patients (23/29). Fig.5A shows the overlapping lesion distribution across anatomical regions. DIFAT and clinical lesions overlapped primarily in the apex (72.0±8.63%) and inferior/inferolateral (73.9±7.84%), partially in anterior/anterolateral (30.1±14.6%), and poorly in septum (1.96±1.22%) (Fig.5A).

Examples of overlapping lesions are shown in Fig.5B. Overlapping lesions localized to the apex for patients 2 and 4, anterior/anterolateral for patient 5, and inferior/inferolateral for patients 7 and 8 (Fig.5B). Patients 9, 10, and 11 had extensive clinical ablations spanning both the inferior/inferolateral and apex; correspondingly, overlapping lesions occurred in both the inferior/inferolateral and apex.

DIFAT predicts VTs targeted in redo ablation procedures

DIFAT predicted VTs targeted in redo ablation procedures years after the index procedure. Ten out of 29 patients had more than one VT ablation procedure at least a month apart. Seven of these patients with VT recurrence had redo ablations performed in the same location as their index procedure, indicating that VT recurrence could have resulted from ineffective lesions. The remaining 3 patients (1, 3, and 6) had redo procedures ~4 years later with ablation sites different from those in the index procedure. To illustrate the change in substrate, voltage maps for both index and redo procedures for these patients are shown in Supplementary Fig.7.

For these 3 patients, we compared the location of index and redo ablations with the DIFAT targets, shown in Fig.6. For patient 1, index ablations were delivered basal inferiorly, whereas redo ablations were delivered mid inferiorly. DIFAT predicted 3 targets: one coinciding with index ablations (Fig.6, top left) and two others that aligned well with redo ablations (Fig.6, top right). For patient 3, the left DIFAT targets co-localized with index ablations (Fig.6, middle left) whereas the right DIFAT targets coincided with redo ablations (Fig.6, middle right). For patient 6, DIFAT targets partially co-localized with index ablations (Fig.6, bottom left); however, DIFAT's predictions matched well both sets of extensive redo ablations (Fig.6, bottom right). These results demonstrate DIFAT's ability to complement index ablation strategies to prevent VT recurrence.

Discussion

This study presented DIFAT, a digital-heart technology that incorporates post-infarct inFAT distribution from CT to predict individualized VT ablation targets in ICM patients. DIFAT non-invasively assesses the arrhythmogenic propensity of the inFAT-based substrate and

determines the possible locations where VTs could perpetuate; these locations constitute the first-round digital ablation targets that would eliminate the ability of the patient's inFAT-based substrate to sustain VT. However, as ablation creates a new substrate comprised of residual native remodeling and ablation lesions, emergent VTs could manifest in the digital heart. DIFAT is designed to capture the locations where emergent VTs perpetuate in the digital heart, targeting of which then becomes part of the final DIFAT ablation strategy, with targets to be exported for EAM navigation. Thus, the DIFAT technology could be viewed as a third type of ablation strategy different from both modifying the substrate and targeting of mappable VTs, a "focused substrate-based VT ablation" approach; the difference is that only locations found to sustain VTs in the digital hearts are targeted, rather than electrophysiological abnormalities in the substrate, such as scar homogenization[1], isochronal crowding[4], and late abnormal ventricular activity.[23]

DIFAT has also a unique advantage in that it relies on CT, a widely accessible imaging modality, which renders DIFAT implementable at a broad range of centers without LGE-CMR expertise, and for patients with ICDs. DIFAT ablation targets can easily be imported into EAM systems in real-time to guide ablation procedures, the methodology for which has been validated in our previous studies.[6,24] Because DIFAT technology is digital, it could factor in the predicted ablation strategy, anatomical constraints and restrict delivery of DIFAT lesions to only endocardium or epicardium, rather than anywhere within the myocardium. Furthermore, DIFAT could highlight regions in the inFAT-based substrate that require reinforcing ablation lesions. Thus, prospective implementation of DIFAT could potentially improve VT ablation therapeutic precision and decrease VT recurrence rates, reducing the burden of costly redo ablations. The present retrospective study assessed the predictive capabilities of the technology by comparing DIFAT ablation targets to clinical data from 29 patients with ICM, all with ICDs. DIFAT ablations not only co-localized with index ablations in most cases, but also with redo ablations in 3 patients, highlighting the potential for DIFAT to address incomplete ablation strategies.

inFAT creates arrhythmogenic substrate for VT

Prior studies demonstrate that inFAT is associated with VT. In a retrospective study of patients with ICM, inFAT on CE-CT was more prevalent in those with VT than those without VT.[13] inFAT localizes to infarcted tissue[25] and often develops years after the infarct[10] consistent with the timescale of post-infarct VTs development. Importantly, critical VT circuits co-localized with regions of inFAT in both experimental[12] and clinical studies.[13] Consistent with these findings, the digital-heart technology predicted VT circuits arising from the inFAT-based substrate.

A recent study demonstrated that inFAT is an independent predictor of post-infarct VT recurrence.[14] Consistent with this study, DIFAT predicted VTs that were targeted in redo procedures, suggesting that the index ablation incompletely addressed these patients' VT burden. inFAT may predict VT recurrence because adipose tissue, as an insulator, significantly interferes with proper lesion formation from radiofrequency ablation. Certain critical sites that are found to be embedded in the inFAT-based substrate would warrant

greater attention. Thus, DIFAT could guide, in real time, the delivery of reinforcing lesions to these regions.

Distribution of DIFAT lesions

Overlapping DIFAT and clinical lesions predominantly localized to the apex and not to the septum. This resulted from the fact that the greatest inFAT amount was found in the apex while the least was in the septum, consistent with prior studies.[11,25] It is unknown why there is a low prevalence of septal inFAT. inFAT correlates with large scars[14] suggesting that its development may be a compensatory response promoting wound healing in severe infarcts that occurs over years. Because the septum has dual vascular supplies from both the posterior descending and left anterior descending arteries, it may have better healing post-infarct which may limit compensatory adipogenesis, thereby resulting in less septal inFAT. This implies that DIFAT is not suitable for predicting critical VT sites in base/mid septum. Despite this limitation, DIFAT still predicted VTs originating from a variety of non-septal locations and identified targets not addressed during index ablations, highlighting its potential utility.

Comparison of inFAT to other substrates

CE-CT provides excellent spatial resolution of the myocardial wall but cannot directly characterize myocardial scar distribution. DIFAT targets are based on the inFAT substrate only and not on non-fat infiltrated scar. Future studies will be needed to evaluate the arrhythmogenicity of scar-based substrate on LGE-CMR versus inFAT-based substrate on CE-CT.

Wall thinning on CE-CT has been investigated as a surrogate of myocardial scar;[9] it correlates with altered electrograms and VT ablations.[9] However, wall thickness is a single-value parameter at a given location that does not vary transmurally, thus it cannot provide information about the 3D structure of VT circuits. Recent research has provided ample evidence of VT pathways located within the midmyocardium.[26] The inFAT and fat-myocardium admixture distributions provide 3D characterization of the mid-myocardial substrate, and DIFAT can uncover midmyocardial VT circuits. In addition to its other advantages, DIFAT might improve therapeutic precision of intramural ablation.[27]

Limitations

Our study has several limitations. First, CT artifacts from ICD leads were present in certain patients. Although our automated image processing workflow removed most of the artifact, residual artifact could remain and be misclassified as inFAT or fat-myocardium admixture. However, all predicted targets were away from artifact, suggesting that it did not affect predictions. Next, because of the lack of experimental data, fat-myocardium admixture electrophysiological properties were approximated with those of infarct border zone. Further work should be done to characterize the effects of inFAT on surrounding ventricular tissue electrophysiology. Third, DIFAT is not suitable for patients without inFAT such as those with younger infarct ages.[11] Lastly, although our results suggested that DIFAT is feasible in guiding VT ablation, our clinical validation relied on comparisons with electrically-defined

scar and clinical ablation lesions because annotated critical sites were not readily available in this cohort.

Conclusions

Here, we present DIFAT, a non-invasive, personalized digital-heart technology that uses inFAT identified on CT to predict optimal VT ablation targets. It is designed to render the inFAT-based substrate completely non-inducible for VT. We successfully tested the feasibility of DIFAT in a retrospective cohort of 29 patients with post-infarct VTs. Not only were DIFAT ablation targets smaller than the co-localized index ablations, but the technology also predicted redo ablation targets, highlighting its ability to complement index ablation strategies. DIFAT's reliance on CT makes it suitable for both patients with ICDs (as in this retrospective cohort) and without, and for centers without LGE-CMR expertise. Because high-quality CT images are reliably obtained, DIFAT can be readily incorporated into VT ablation workflows. As DIFAT is designed to precisely target all possible locations capable of sustaining VTs, the expectation is that it will augment VT ablation efficacy and mitigate expensive redo ablation procedures. Prospective studies will be needed to fully demonstrate DIFAT's capabilities.

Supplementary Material

Refer to Web version on PubMed Central for supplementary material.

Acknowledgments

Sources of Funding: This work was supported by funding from the National Institutes of Health R01-HL142893 to SN and NT, R01-HL142496 and R01HL126802 to NT, and a grant from the Leducq Foundation to NT.

Nonstandard Abbreviations and Acronyms

inFAT	infiltrating adipose tissue
VAAT	Virtual-heart Arrhythmia Ablation Targeting
DIFAT	Digital-heart Identification of Fat-based Ablation Targeting
VT	ventricular tachycardia
ICM	ischemic cardiomyopathy
ICD	implantable cardioverter defibrillator
LGE-CMR	late-gadolinium-enhanced cardiac magnetic resonance
CE-CT	contrast-enhanced computed tomography
EAM	electroanatomic map/mapping
LV	left ventricle
RV	right ventricle

3D	three-dimensional

References

1. Guandalini GS, Liang JJ, Marchlinski FE. Ventricular Tachycardia Ablation: Past, Present, and Future Perspectives. JACC Clin Electrophysiol. 2019;5:1363–1383. [PubMed: 31857035]
2. Marchlinski FE, Haffajee CI, Beshai JF, Dickfeld TML, Gonzalez MD, Hsia HH, Schuger CD, Beckman KJ, Bogun FM, Pollak SJ, et al. Long-term success of irrigated radiofrequency catheter ablation of sustained ventricular tachycardia: Post-approval THERMOCOOL VT trial. J Am Coll Cardiol. 2016;67:674–683. [PubMed: 26868693]
3. Yokokawa M, Desjardins B, Crawford T, Good E, Morady F, Bogun F, Arbor A. Heart Rhythm Disorders Reasons for Recurrent Ventricular Tachycardia After Catheter Ablation of Post-Infarction Ventricular Tachycardia. J Am Coll Cardiol. 2013;61:66–73. [PubMed: 23122796]
4. Aziz Z, Shatz D, Raiman M, Upadhyay GA, Beaser AD, Besser SA, Shatz NA, Fu Z, Jiang R, Nishimura T, et al. Targeted Ablation of Ventricular Tachycardia Guided by Wavefront Discontinuities During Sinus Rhythm: A New Functional Substrate Mapping Strategy. Circulation. 2019;140:1383–1397. [PubMed: 31533463]
5. Mahida S, Sacher F, Dubois R, Sermesant M, Bogun F, Haïssaguerre M, Jaïs P, Cochet H. Cardiac Imaging in Patients with Ventricular Tachycardia. Circulation. 2017;136:2491–2507. [PubMed: 29255125]
6. Prakosa A, Arevalo HJ, Deng D, Boyle PM, Nikolov PP, Ashikaga H, Blauer JJE, Ghafoori E, Park CJ, Blake RC, et al. Personalized virtual-heart technology for guiding the ablation of infarct-related ventricular tachycardia. Nat Biomed Eng. 2018;2:732–740. [PubMed: 30847259]
7. Esposito A, Palmisano A, Antunes S, Maccabelli G, Colantoni C, Rancoita PMV, Baratto F, Di Serio C, Rizzo G, De Cobelli F, et al. Cardiac CT With Delayed Enhancement in the Characterization of Ventricular Tachycardia Structural Substrate. JACC Cardiovasc Imaging. 2016;9:822–832. [PubMed: 26897692]
8. Mendoza DD, Joshi SB, Weissman G, Taylor AJ, Weigold WG. Viability imaging by cardiac computed tomography. J Cardiovasc Comput Tomogr. 2010;4:83–91. [PubMed: 20430338]
9. Ghannam M, Cochet H, Jais P, Sermesant M, Patel S, Siontis KC, Morady F, Bogun F. Correlation between computer tomography-derived scar topography and critical ablation sites in postinfarction ventricular tachycardia. J Cardiovasc Electrophysiol. 2018;29:438–445. [PubMed: 29380921]
10. Ichikawa Y, Kitagawa K, Chino S, Ishida M, Matsuoka K, Tanigawa T, Nakamura T, Hirano T, Takeda K, Sakuma H. Adipose Tissue Detected by Multislice Computed Tomography in Patients After Myocardial Infarction. JACC Cardiovasc Imaging. 2009;2:548–555. [PubMed: 19442939]
11. Raney AR, Saremi F, Kenchaiah S, Gurudevan SV, Narula J, Narula N, Channual S. Multidetector computed tomography shows intramyocardial fat deposition. J Cardiovasc Comput Tomogr. 2008;2:152–163. [PubMed: 19083940]
12. Pouliopoulos J, Chik WWB, Kanthan A, Sivagangabalan G, Barry MA, Fahmy PNA, Midekin C, Lu J, Kizana E, Thomas SP, et al. Intramyocardial Adiposity After Myocardial Infarction. Circulation. 2013;128:2296–2308. [PubMed: 24036606]
13. Sasaki T, Calkins H, Miller CF, Zviman MM, Zipunnikov V, Arai T, Sawabe M, Terashima M, Marine JE, Berger RD, et al. New insight into scar-related ventricular tachycardia circuits in ischemic cardiomyopathy: Fat deposition after myocardial infarction on computed tomography--A pilot study. Heart Rhythm. 2015;12:1508–1518. [PubMed: 25814415]
14. Cheniti G, Sridi S, Sacher F, Chaumeil A, Pillois X, Takigawa M, Frontera A, Vlachos K, Martin CA, Teijeira E, et al. Post-Myocardial Infarction Scar With Fat Deposition Shows Specific Electrophysiological Properties and Worse Outcome After Ventricular Tachycardia Ablation. J Am Heart Assoc. 2019;8:e012482. [PubMed: 31378121]
15. Aliyari Ghasabeh M, Te Riele ASJM, James CA, Chen HSV, Tichnell C, Murray B, Eng J, Kral BG, Tandri H, Calkins H, et al. Epicardial Fat Distribution Assessed with Cardiac CT in Arrhythmogenic Right Ventricular Dysplasia/Cardiomyopathy. Radiology. 2018;289:641–648. [PubMed: 30129902]

16. Arevalo HJ, Vadakkumpadan F, Guallar E, Jebb A, Malamas P, Wu KC, Trayanova NA. Arrhythmia risk stratification of patients after myocardial infarction using personalized heart models. Nat Commun. 2016;7:11437. [PubMed: 27164184]
17. Borkan GA, Gerzof SG, Robbins AH, Hults DE, Silbert CK, Silbert JE. Assessment of abdominal fat content by computed tomography. Am J Clin Nutr. 1982;36:172–177. [PubMed: 7091027]
18. Bayer JD, Blake RC, Plank G, Trayanova NA. A novel rule-based algorithm for assigning myocardial fiber orientation to computational heart models. Ann Biomed Eng. 2012;40:2243–2254. [PubMed: 22648575]
19. Ustunkaya T, Desjardins B, Liu B, Zahid S, Park J, Saju N, Trayanova N, Zimmerman SL, Marchlinski FE, Nazarian S. Association of regional myocardial conduction velocity with the distribution of hypoattenuation on contrast-enhanced perfusion computed tomography in patients with postinfarct ventricular tachycardia. Heart Rhythm. 2019;16:588–594. [PubMed: 30935494]
20. Nattel S, Maguy A, Le Bouter S, Yeh YH. Arrhythmogenic ion-channel remodeling in the heart: Heart failure, myocardial infarction, and atrial fibrillation. Physiol. Rev. 2007;87:425–456. [PubMed: 17429037]
21. Shade JK, Cartoski MJ, Nikolov P, Prakosa A, Doshi A, Binka E, Olivieri L, Boyle PM, Spevak PJ, Trayanova NA. Ventricular arrhythmia risk prediction in repaired Tetralogy of Fallot using personalized computational cardiac models. Heart Rhythm. 2020;17:408–414. [PubMed: 31589989]
22. Gerstenfeld EP. Recurrent ventricular tachycardia after catheter ablation in post-infarct cardiomyopathy: “Failure” of ablation or progression of the substrate? J Am Coll Cardiol. 2013;61:74–76. [PubMed: 23122794]
23. Jaïs P, Maury P, Khairy P, Sacher F, Nault I, Komatsu Y, Hocini M, Forclaz A, Jadidi AS, Weerasooryia R, et al. Elimination of local abnormal ventricular activities : A new end point for substrate modification in patients with scar-related ventricular tachycardia. Circulation. 2012;125:2184–2196. [PubMed: 22492578]
24. Boyle PM, Zghaib T, Zahid S, Ali RL, Deng D, Franceschi WH, Hakim JB, Murphy MJ, Prakosa A, Zimmerman SL, et al. Computationally guided personalized targeted ablation of persistent atrial fibrillation. Nat Biomed Eng. 2019;3:870–879. [PubMed: 31427780]
25. Baroldi G, Silver MD, De Maria R, Parodi O, Pellegrini A. Lipomatous metaplasia in left ventricular scar. Can J Cardiol. 1997;13:65–71. [PubMed: 9039067]
26. Tung R, Raiman M, Liao H, Zhan X, Chung FP, Nagel R, Hu H, Jian J, Shatz DY, Besser SA, et al. Simultaneous Endocardial and Epicardial Delineation of 3D Reentrant Ventricular Tachycardia. J Am Coll Cardiol. 2020;75:884–897. [PubMed: 32130924]
27. Stevenson WG, Tedrow UB, Reddy V, AbdelWahab A, Dukkipati S, John RM, Fujii A, Schaeffer B, Tanigawa S, Elsokkari I, et al. Infusion Needle Radiofrequency Ablation for Treatment of Refractory Ventricular Arrhythmias. J Am Coll Cardiol. 2019;73:1413–1425. [PubMed: 30922472]

What Is Known?

- Post-infarct hearts often have infiltrating adipose tissue (inFAT) that forms an arrhythmogenic substrate, predisposing patients with ischemic cardiomyopathy to ventricular tachycardias (VT).
- Digital-heart technology has been previously developed for incorporating patient-specific scar distribution from late-gadolinium-enhanced magnetic resonance imaging for personalized ablation targeting of ventricular arrhythmias.

What the Study Adds?

- Digital-heart Identification of Fat-based Ablation Targeting (DIFAT) is a novel, computationally-driven technology that predicts VT ablation targets based on the inFAT-based substrate derived from computed tomography applicable for patients with and without implantable cardioverter defibrillators.
- Incorporation of DIFAT into clinical workflows may help improve index VT ablation precision and reduce the burden of redo procedures.

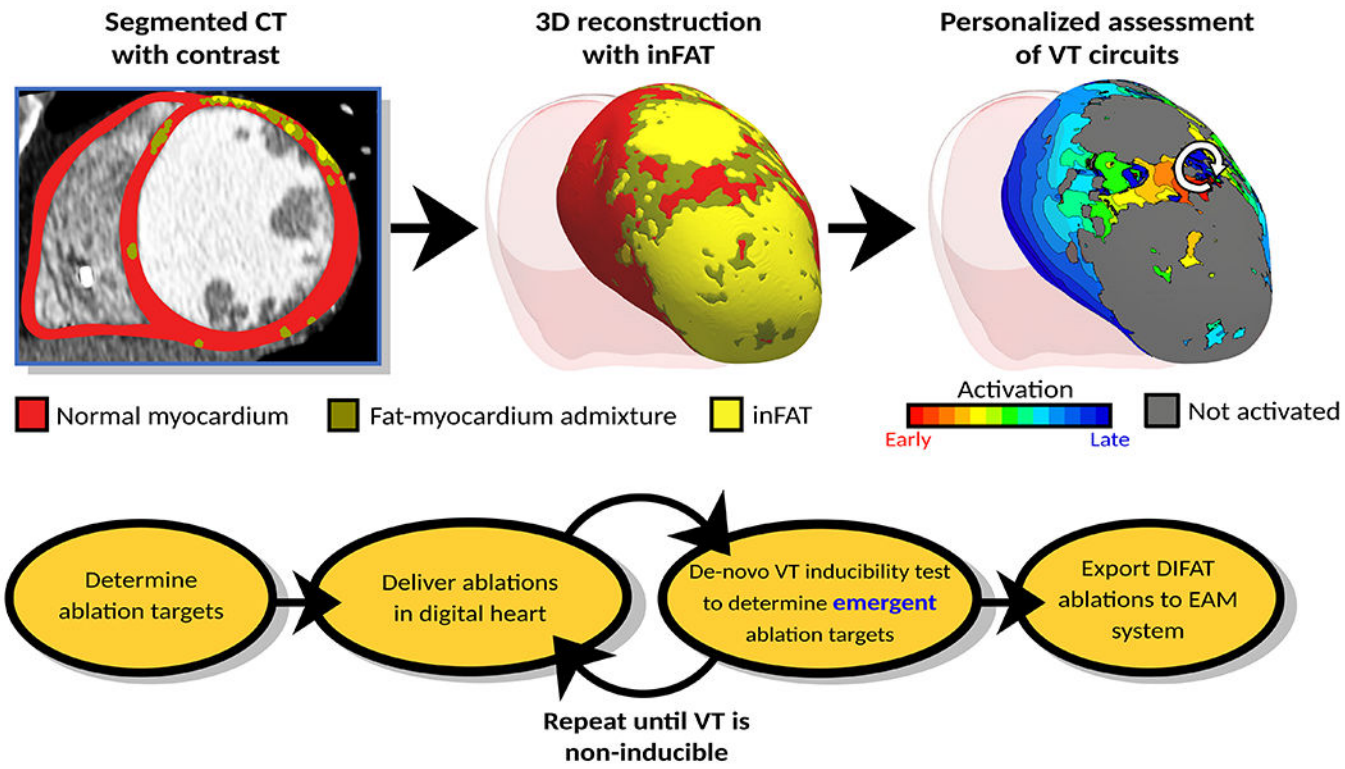

Figure 1:

DIFAT Workflow. *Top:* From computed tomographic images with contrast, the myocardium is segmented into non-injured myocardium, inFAT, and fat-myocardium admixture. Personalized 3D digital hearts are reconstructed from this segmented data and electrophysiological information. inFAT-based arrhythmogenic propensity is assessed to identify all possible VTs the substrate can sustain. White arrow represents direction of induced reentrant propagation. *Bottom:* All VTs induced in the inFAT-based substrate are analyzed to determine minimum-size ablation targets. These ablation lesions are incorporated in the digital hearts as a mock-up of the clinical procedure. VT inducibility in the post-ablation digital hearts is tested again to determine whether emergent VTs arise in the new substrate. This process is repeated until complete VT non-inducibility is achieved in the personalized digital heart. The DIFAT ablations can then be imported into an EAM system to guide augment the ablation procedure. DIFAT: Digital-heart Identification of Fat-based Ablation Targets, EAM=electroanatomic mapping, inFAT=infiltrating adipose tissue, VT=ventricular tachycardia

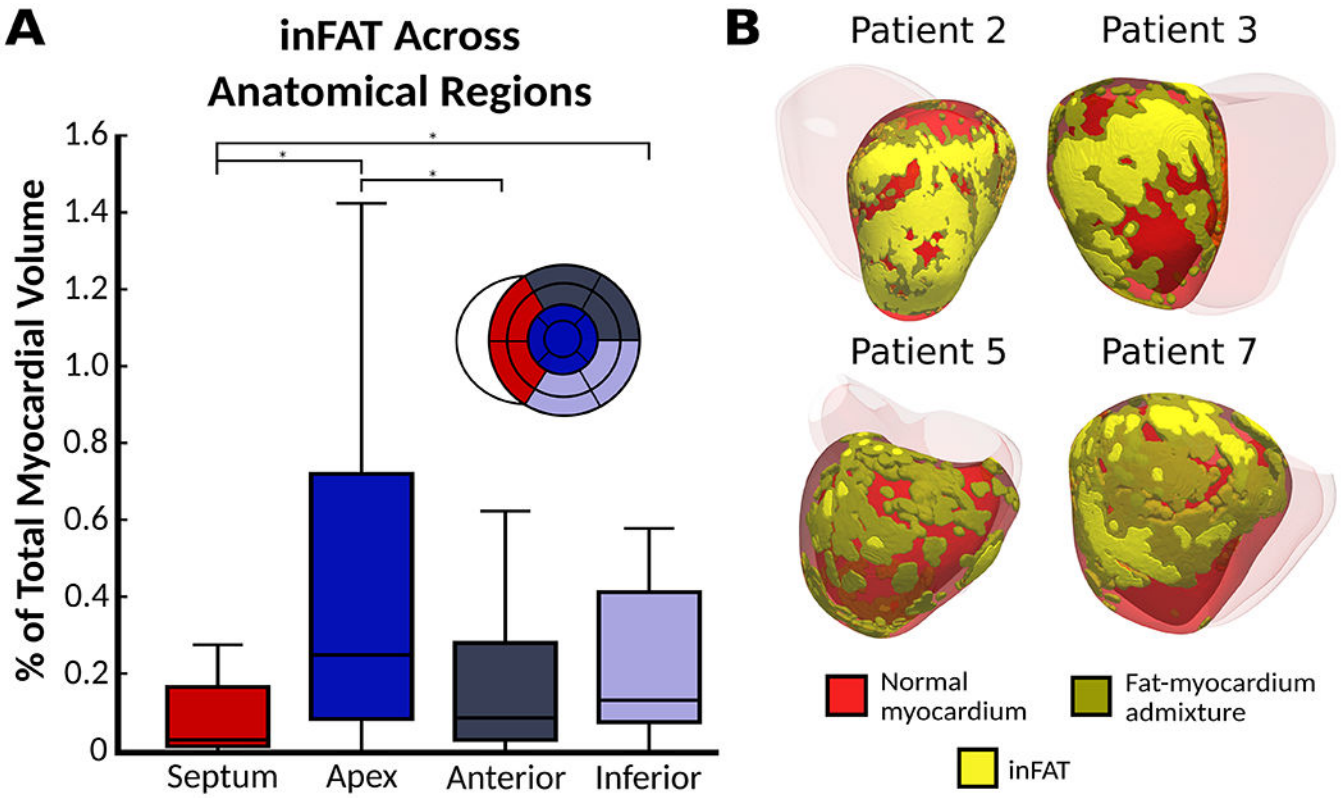

Figure 2:

inFAT distributions across patient hearts. **(A)** Quantification of inFAT across all patient hearts. Box plots denote the median amount of inFAT as a percentage of myocardium volume. **(B)** Examples of varying inFAT and fat-myocardium admixture distributions in 4 patients. Abbreviations as in Fig.1.

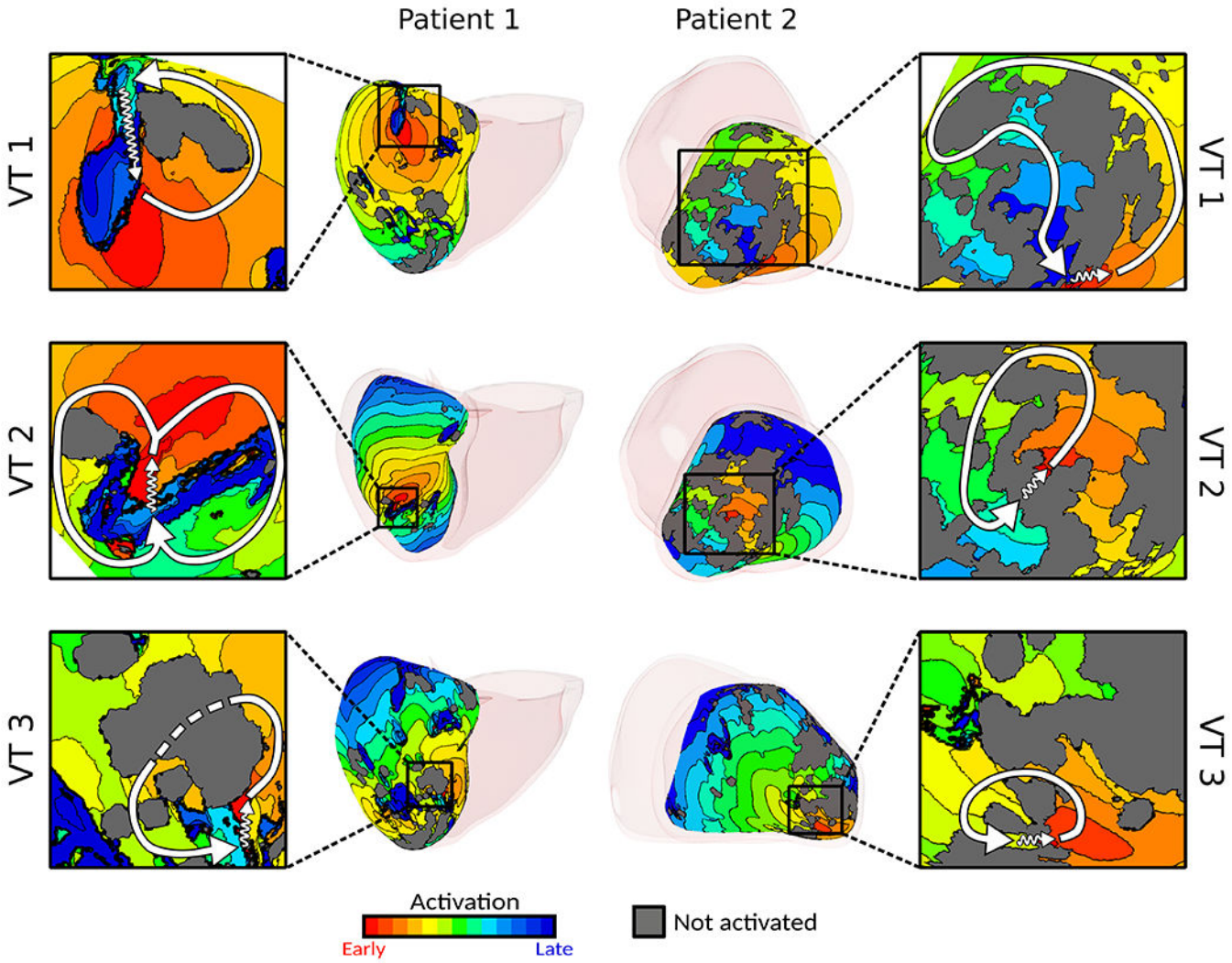

Figure 3:

Digital-heart simulations predict potential VTs. Examples of VTs in digital hearts of patients 1 and 2. Insets present detail of activation; white arrows denote re-entrant pathway, zigzag arrows denote conduction channels, and dashed line (patient 1 VT 3) denotes conduction below non-activated tissue. For patient 1, activation maps for VT 1 and VT 3 depict the epicardial surface whereas the activation map for VT2 depicts the endocardial activation map. For patient 2, all activation maps shown depict the endocardial surface. Abbreviations as in Fig.1.

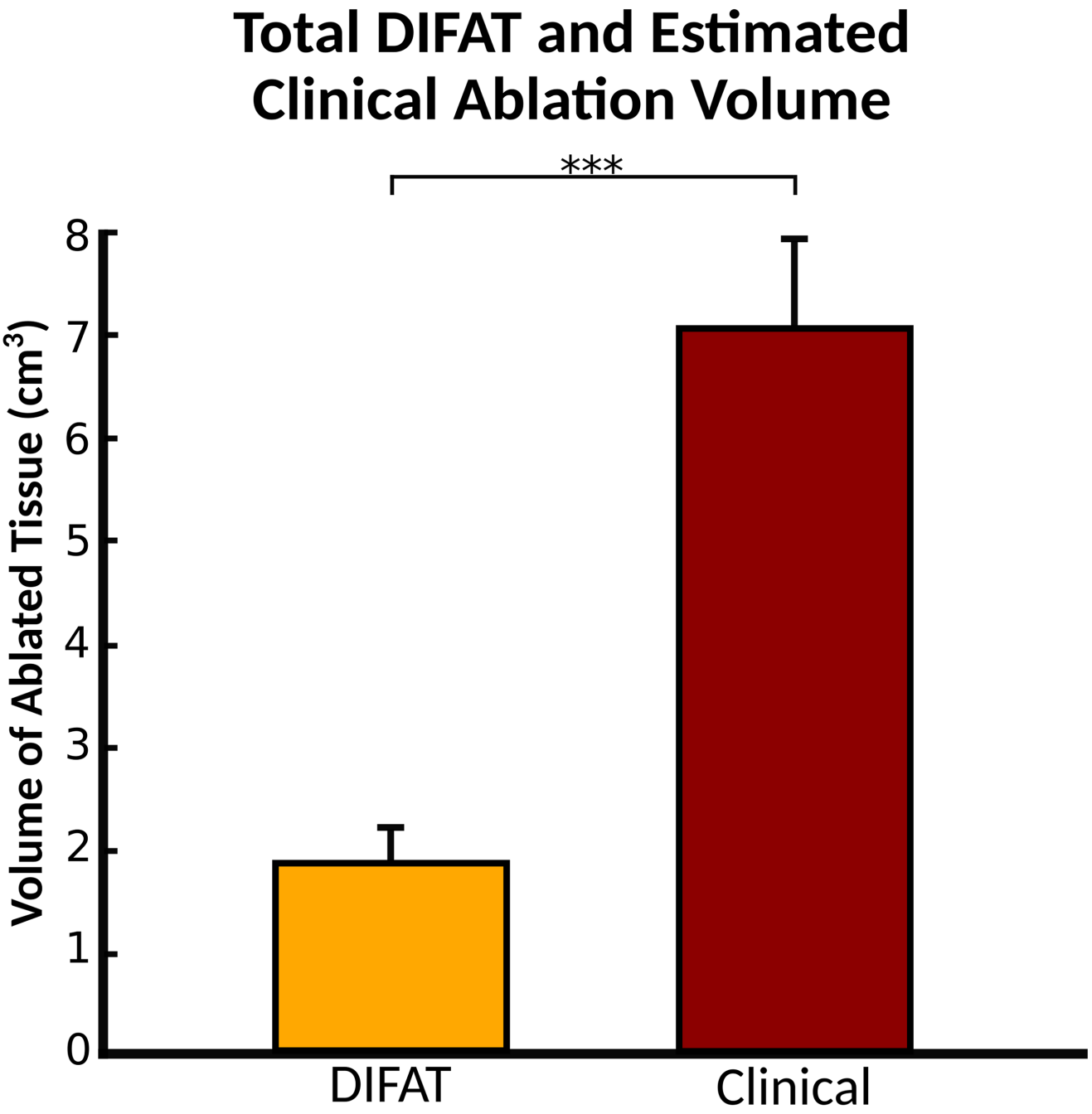

Figure 4:

Comparison between DIFAT ablation targets volume and estimated clinical ablation lesion volumes. The volume of DIFAT lesions was significantly smaller than that of the clinical ablations ($p<0.0005$, paired t-test). The mean volume of DIFAT ablated tissue was 1.87+/−0.35 cm^3 whereas the mean volume of estimated clinical ablations was 7.05 +/−0.88 cm^3. Abbreviations as in Fig.1.

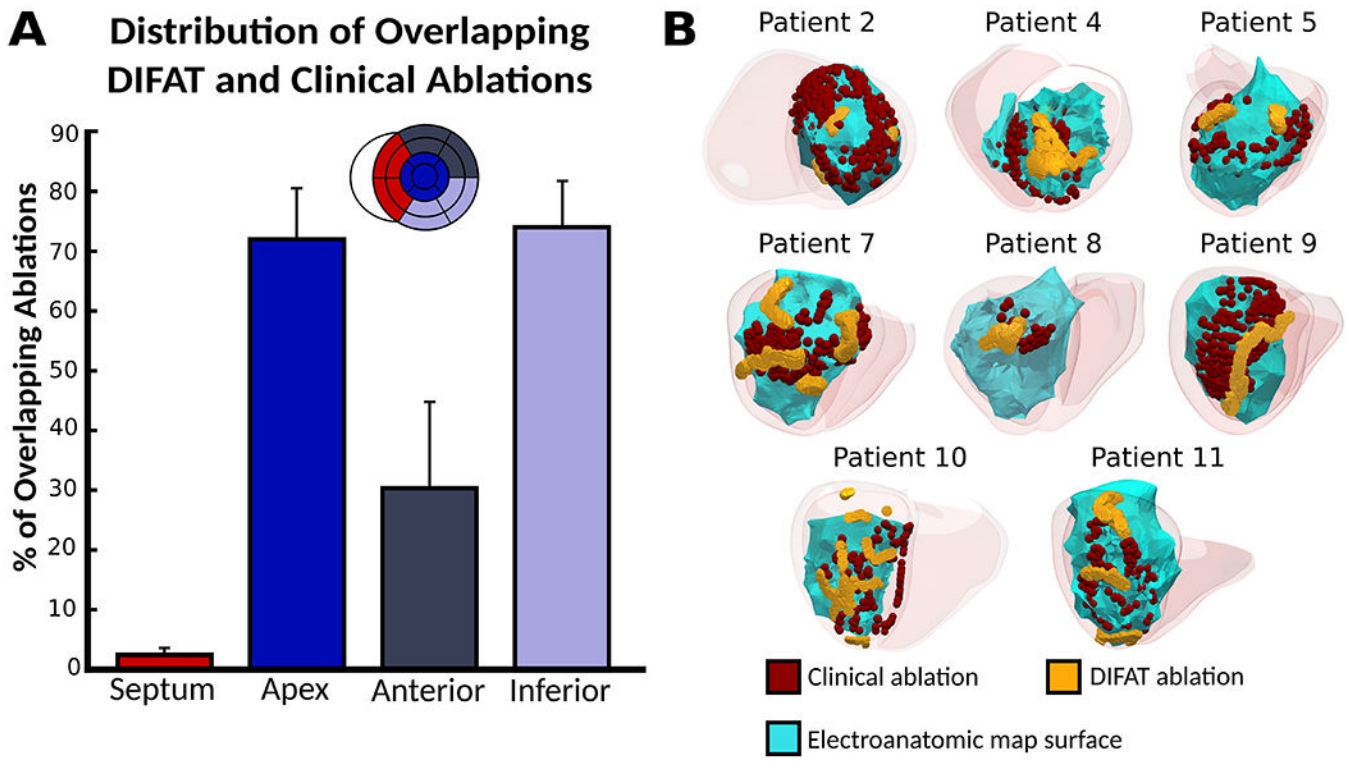

Figure 5:

DIFAT ablations co-localize with clinical ablation lesions. **(A)** Distribution of overlapping DIFAT and clinical ablation lesions across anatomical regions. Bars denote mean percentage of overlapping lesions across patients. **(B)** Examples of co-localizing lesions for 8 patients. Abbreviations as in Fig.1.

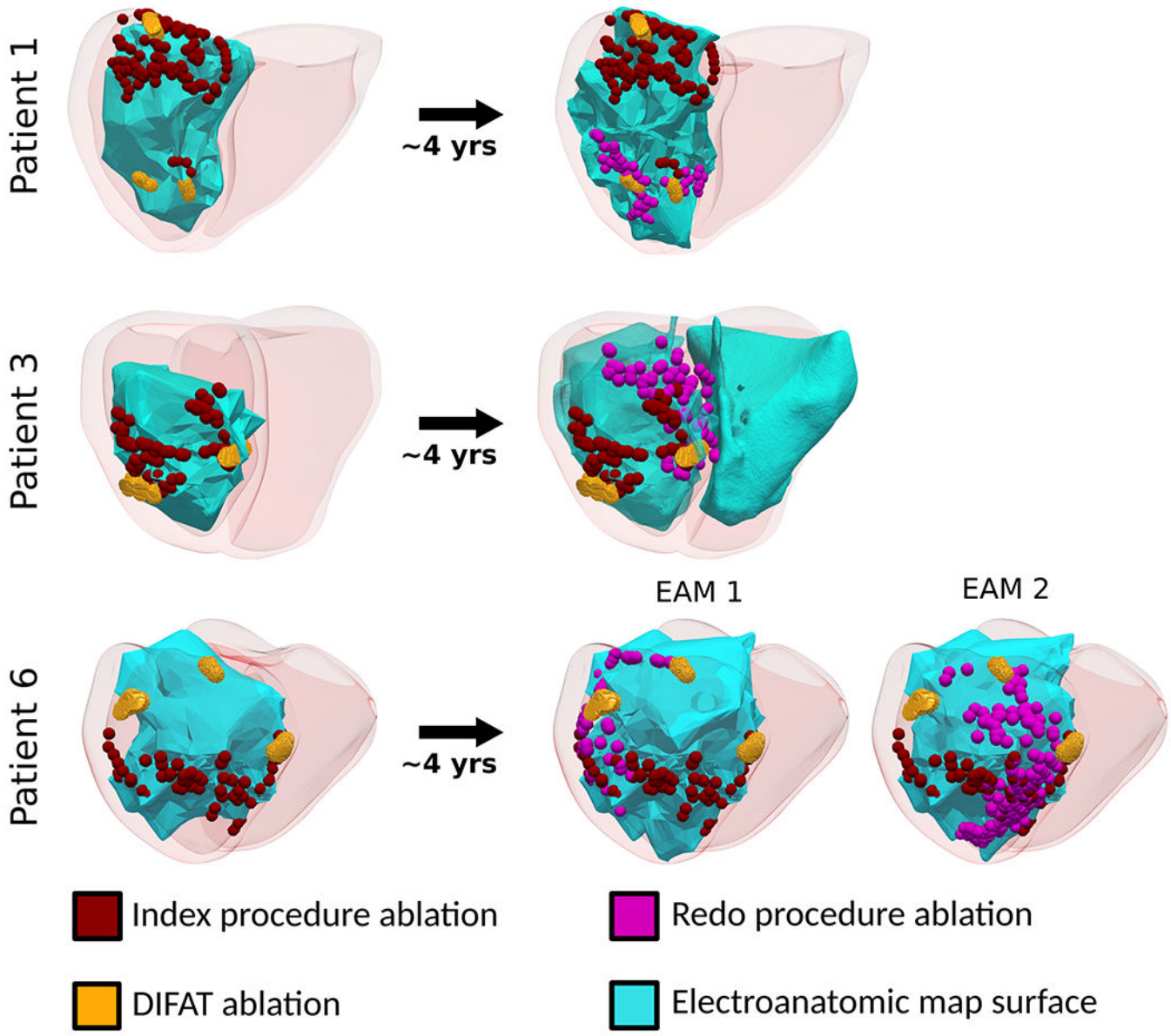

Figure 6:

DIFAT predicts redo ablation targets. Co-localizing DIFAT and clinical ablation lesions for three patients who underwent redo ablations ~4 years after their index procedure. Abbreviations as in Fig.1.

Table 1:

Baseline characteristics of patients enrolled in the study

Patient Characteristics	Patients (N = 29)
Age, y	63 (12)
Infarct age, y	18.5 (11.25)
Male	21 (72.4%)
ICD implanted	29 (100%)
LVEF, %	30 (15)
# of substrate-based ablation procedures	27 (93.1%)
# VTs induced in procedure	3 (2)
Infarct Location	
Anterior/Anteroseptal	11 (37.9%)
Inferior	11 (37.9%)
Lateral	5 (17.2%)
Unknown	2 (6.9%)

*Categorical variables are expressed as the count (percentage). Continuous and ordinal variables are expressed as median (25^{th} – 75^{th} interquartile range).

†Abbreviations: VT: ventricular tachycardia, LVEF: left ventricular ejection fraction, ICD: implantable cardioverter defibrillator